sciendo

DOI 10.2478/ama-2023-0025

acta mechanica et automatica, vol.17 no.2 (2023)
Special Issue "Modern Trends in Automation and Robotics in tribute to Professor Tadeusz Kaczorek"

FINITE LENGTH TRIPLE ESTIMATION ALGORITHM AND ITS APPLICATION TO GYROSCOPE MEMS NOISE IDENTIFICATION

Michal MACIAS*, Dominik SIEROCIUK*

*Institute of Control and Industrial Electronics, Warsaw University of Technology, ul. Koszykowa 75, 00–662 Warsaw, Poland

michal.macias@pw.edu.pl, dominik.sierociuk@pw.edu.pl

received 31 October 2022, revised 26 December 2022, accepted 4 January 2023

Abstract: The noises associated with MEMS measurements can significantly impact their accuracy. The noises characterised by random walk and bias instability errors strictly depend on temperature effects that are difficult to specify during direct measurements. Therefore, the paper aims to estimate the fractional noise dynamics of the stationary MEMS gyroscope based on finite length triple estimation algorithm (FLTEA). The paper deals with the state, order and parameter estimation of fractional order noises originating from the MEMS gyroscope, being part of the popular Inertial Measurement Unit denoted as SparkFun MPU9250. The noise measurements from x, y and z gyroscope axes are identified using a modified triple estimation algorithm (TEA) with finite approximation length. The TEA allows a simultaneous estimation of the state, order and parameter of fractional order systems. Moreover, as it is well-known that the number of samples in fractional difference approximations plays a key role, we try to show the influence of applying the TEA with various approximation length constraints on final estimation results. The validation of finite length TEA in the noise estimation process coming from MEMS gyroscope has been conducted for implementation length reduction achieving 50% of samples needed to estimate the noise with no implementation losses. Additionally, the capabilities of modified TEA in the analysis of fractional constant and variable order systems are confirmed in several numerical examples.

Key words: fractional calculus, fractional Kalman filter, estimation of fractional order systems, fractional order noise

1. INTRODUCTION

The fractional calculus (FC) is, in itself, an extension of traditional differential and integral calculus. The differential orders in FC can be real or even complex numbers. The fractional derivative appeared for the first time in the correspondence between Leibniz and l'Hôpital in 1695, and thereby, it appeared almost simultaneously with the integer order calculus. The theoretical background for this calculus can be found in several already classic works in the literature [1, 2, 3, 4, 6]; additionally, in multiple relatively recently published books [7,8], some applications of this calculus have been explored.

The main advantage of fractional order operators in comparison to the integer order case is that the fractional order derivatives depend not only on local time conditions but also on the whole past of the function [10]. This property can be especially useful for the description of dynamics possess with a long-term memory nature. The FC was found to be especially efficient in modelling diffusive systems [11, 12, 13, 14]. For example, in the heat transfer process of the solid beam, it is possible to describe dynamics between temperature and heat flux at the desired point as a half-order integral. When the heated material is not solid (heterogeneous), the order of the integration can be different by half, as was presented in the study of Sierociuk et al. [11].

The FC also allows the construction of new types of filters and new tools for signal analysis. Some applications of fractional order calculus in signal processing have been presented in the literature [5, 15, 16, 17]. For constant and variable fractional order systems, some generalisations of the Kalman filter have been presented in the studies of Sierociuk et al. [18], Sierociuk [19] and Sierociuk and Ziubinski [20]. When the uncorrelated noise (such as white noise) passes through a dynamical system, the dynamically correlated noise (coloured noise) is obtained. When the dynamics contain fractional order, a fractional noise is obtained. In the study of Wyss [21], an introduction is presented to fractional order noises (the noises obtained by applying uncorrelated white noise to fractional order dynamics). In the study of Sierociuk and Ziubinski [22], estimation schemes are presented for discrete fractional and integer order state-space systems with fractional order coloured noise. In the latter of these studies, owing to the additional information about noise dynamic used by the estimation algorithm proposed therein, better estimates of the state vector could be obtained.

The MEMS gyroscope sensors are quite complex dynamical systems encompassing non-linear dynamics, external disturbances and thermal noises, especially in high acceleration and high-velocity environments such as space crafts [34], hypersonic vehicles [35], missiles or munition [36]. The use of advanced control algorithms is necessary for a study of the application of nonlinearities in MEMS gyroscopes, especially those involving a hysteresis of quantisation levels.. For example, neural network approaches were used in the studies of Shao et al. [37, 38] and Shao and Shi [39]; additionally, in the study of Shao et al. [40], a fuzzy wavelet neural control was applied. In this paper, only static case noise analysis will be considered, and accordingly the research approach used in the present study would be a special case that omits the influence of sensor externally driven dynamics and focusses only on modelling thermal and other noises that can

be measured when the sensor does not move. Especially, thermal-like noises can be efficiently modelled using fractional order models (fractional noises), which is the main motivation for applying fractional order estimation tools and undertaking investigation of static noise cases.

In practical fractional noise estimation, there is a problem with properly determining the parameters and order of the noise. In the study of Sierociuk and Macias [23], the triple estimation algorithm (TEA) for state vector, order and system parameters' estimation was proposed and described in detail. In the study of Macias et al. [24], a triple estimation algorithm was used to carry out identification of fractional order noise in MEMS accelerometer measurements. In the practical application of the triple estimation algorithm, it was found that the algorithm requires quite a high numerical power. The principal difficulty lies in the realisation of fractional order differences when the full number of samples is used.The problem of direct application of fractional order difference resulting in a high numerical power consumption is a well-recognised one in the literature, and there have been multiple studies proposing other methods characterised by much lower levels of numerical power consumption. In Stanisławski et al. [25,26], some types of approximations including Laguerre-based differences were proposed and analysed. The most typical method of approximation is to reduce the number of samples that are considered, which has an influence on derivative accuracy.

The paper's novelty lies in its modification of the triple estimation algorithm by introducing a limited number of samples during computation. Then, the new algorithm will be applied in the identification of the state, order and parameter of the gyroscope's x, y and z axes' noises as part of the Inertial Measuring Unit denoted by MPU9250. Moreover, the results will be compared to each other considering the various implementation lengths of FLTEA. So, in contrast with the approaches used in the studies of Sierociuk and Ziubinski [22] and Sierociuk and Macias [23], we present the triple estimation algorithm with finite length approximation and its application to the gyroscope's noises' estimation. The numerical power consumption of the proposed algorithm has also been analysed.

The remainder of the paper is organised as follows: Section 2 recalls the fractional noises' definition and particular fractional order definition with finite length approximation. In Section 3, the modified TEA with approximation length constraints is presented. Finally, Sections 4 and 5 show the possibilities of TEA in several numerical examples and during the estimation process of noise data originating from the gyroscope's built-in MEMS technology.

2. FRACTIONAL CALCULUS AND FRACTIONAL NOISES

In FC, the three most popular definitions of fractional constant order integral and derivative are used, namely, Grünwald–Letnikov, Riemann–Liouville and Caputo. These definitions possess different properties and may be applied in various areas of engineering.

In this paper, we use the Grünwald–Letnikov definition, which is usually used in discrete systems, as a base for fractional variable order (FVO) difference definition. Due to the applied nature of this work, we will use a discrete approximation of the Grünwald–Letnikov derivative with a finite (not going to 0) sampling time h. Hence, we have the constant order difference definition, which is formulated as the following:

$$ {}_0\Delta_k^\alpha x_k \equiv \sum_{j=0}^{k} \frac{1}{h^\alpha}(-1)^j \binom{\alpha}{j} x_{k-j}, $$

where

$$ \binom{\alpha}{j} \equiv \begin{cases} 1 & \text{for} \quad j = 0, \\ \dfrac{\alpha(\alpha-1)\dots(\alpha-j+1)}{j!} & \text{for} \quad j > 0, \end{cases} $$

$\alpha \in \mathbb{R}$ is a fractional order and h is a time sampling.

Since the estimation of the order will be processed in time, this leads us to variable order operators. Four switching schemes and their equivalence to four definitions of FVO derivatives are presented in the literature [27, 28, 29]. In our paper, we will use the following FVO type of difference:

$$ {}_0^{\mathcal{A}}\Delta_k^{\alpha_k} x_k \equiv \sum_{j=0}^{k} \frac{(-1)^j}{h^{\alpha_k}} \binom{\alpha_k}{j} x_{k-j} $$

where $\alpha_k \in \mathbb{R}$ is FVO.

3. FRACTIONAL NOISE

The time-correlated (coloured) noises are the noises that contain a dynamic correlation between the noise samples. Such noises can be obtained when some noise (uncorrelated) is passed through dynamical systems. For example, electromagnetic field noise can induct some current in an electronic circuit, leading to some dynamically correlated noise in voltage because of some dynamic between current and voltage. When the order of the dynamics is an integer, we will have a dynamically correlated integer order noise, which the following relation can describe:

$$ x_{k+1} = f x_k + \omega_k, $$

where x_k is a time-correlated noise, and ω_k is an uncorrelated noise, for example, white Gaussian noise.

When the dynamics of the system are fractional, for example, in temperature transport (for ideal beam temperature is half order integral of heat flux [11]), the uncorrelated heat flux noise can lead to fractional order dynamically correlated noise in temperature. The coloured fractional order noise is given as follows:

$$ \begin{aligned} {}_0\Delta_{k+1}^\alpha x_{k+1} &= f x_k + \omega_k \\ x_{k+1} &= h^\alpha \, {}_0\Delta_{k+1}^\alpha x_{k+1} \\ &\quad - \sum_{j=1}^{k+1} (-1)^j \binom{\alpha}{j} x_{k-j+1}, \end{aligned} $$

where x_k is a fractional coloured noise, α is an order of the noise and ω_k is an uncorrelated noise.

The appearance of FVO noise can be observed in the case wherein the fractional order of the dynamical system is characterised by changes with time (e.g. when the structure of the heated medium changes over time [12]). Depending on the order-switching manner, different definitions can describe such dynamics. For example, for $\mathcal{A}$-type definition, we will have the following FVO noise dynamics:

sciendo
DOI 10.2478/ama-2023-0025
acta mechanica et automatica, vol.17 no.2 (2023)
Special Issue "Modern Trends in Automation and Robotics in tribute to Professor Tadeusz Kaczorek"

$$
\begin{aligned}
{}_0^{\mathcal{A}}\Delta_k^{\alpha_{k+1}} x_{k+1} &= f x_k + \omega_k \\
x_{k+1} &= h^{\alpha_{k+1}}\, {}_0^{\mathcal{A}}\Delta_k^{\alpha_{k+1}} x_{k+1} \\
&\quad - \sum_{j=1}^{k+1} (-1)^j \binom{\alpha_{k+1}}{j} x_{k-j+1}.
\end{aligned}
$$

Identification of the fractional noise in a real application is a complex process because we do not know the order and system parameters of the noise. We also do not have information about dynamically uncorrelated source noise. In the study of Ziubinski and Sierociuk [30], an identification algorithm for fractional noise was presented, but under the assumption that output noise is the only evident fractional order noise. In experimentally obtained noises, we would instead acquire a combination of dynamically correlated and uncorrelated noises, as the following expression describes:

$$y_k = x_k + v_k.$$

That is why, in this article, we use a triple estimation algorithm to identify parameters of fractional order noises.

4. FINITE LENGTH APPROXIMATION

The definition given by Eq. (2) leads to some implementation problems because of the very long tail of samples used for obtaining the value of difference. This resulted in the problems' characterisation by a high number of numerical operations as well as a high degree of memory consumption. In the literature there exist several algorithms using which to arrive at a more numerically efficient fractional difference approximation, among which the studies of Stanisławski et al. [25,26] can be mentioned as prime examples. In our paper, we will use the most popular method, which involves restricting the number of samples considered to some predefined value L, which will be known as the length of implementation. The finite length approximation will have the following form:

$${}_0^{\mathcal{A},L}\Delta_k^{\alpha_k} x_k = \sum_{j=0}^{L(k)} \frac{(-1)^j}{h^{\alpha_k}} \binom{\alpha_k}{j} x_{k-j},$$

where

$$L(k) = \begin{cases} k & \text{if } k < L \\ L & \text{if } k \geq L \end{cases}$$

Naturally, this approximation will have an influence in determining the accuracy of the obtained results, which will depend on used sampling time, time constants of the object and used input signals.

5. FINITE LENGTH TRIPLE ESTIMATION ALGORITHM

The triple estimation algorithm (TEA) allows estimating state vector, system parameters and fractional order simultaneously. In deploying this algorithm, our main idea is to separate the estimation processes used for states, parameters and orders.This separation allows a better adjustment of used filters, making it possible to obtain better estimation results. A detailed introduction of TEA was presented in the study of Sierociuk and Macias [23]. Here, a modification of that algorithm including finite length approximation of fractional order differences will be proposed (FLTEA).

The FLTEA will be defined for the following linear discrete fractional variable order state-space (DFVOSS) $\mathcal{A}$-type system [31] with finite length implementation of difference:

$$
\begin{aligned}
&{}_0^{\mathcal{A},L}\Delta_{k+1}^{\alpha_{k+1}} x_{k+1} = Ax_k + Bu_k + \omega_k, \\
&x_{k+1} = h^{\alpha_{k+1}}\, {}_0^{\mathcal{A},L}\Delta_{k+1}^{\alpha_{k+1}} x_{k+1} \\
&\quad - \sum_{j=1}^{L(k)+1} (-1)^j \binom{\alpha_{k+1}}{j} x_{k-j+} \\
&y_k = Cx_k + v_k,
\end{aligned}
$$

where $u_k \in \mathbb{R}^d$ is a system input; $y_k \in \mathbb{R}^p$ is a system output; $A \in \mathbb{R}^{N\times N}, B \in \mathbb{R}^{N\times d}$ and $C \in \mathbb{R}^{p\times N}$ are the state system, input and output matrices, respectively; $x_k \in \mathbb{R}^N$ is a state vector; and N is a number of state equations.

In the TEA process, the estimations of the FVO, state variables and parameters are divided into three estimation actions (filters). The first filter, KFx, estimates the state variables' vector $\hat{x}_k$ based on estimates of order and system parameters corresponding to the other filters, namely KFo and KFw, respectively. The second, KFw, estimates the vector of system parameters $\hat{w}_k$ based on state variable and order estimates obtained in the remaining two filters KFx and KFo, respectively. The third filter, KFo, estimates the FVO with the knowledge of state variable and system parameters from filters KFx and KFw, respectively. The scheme of the TEA is given in Fig. 1.

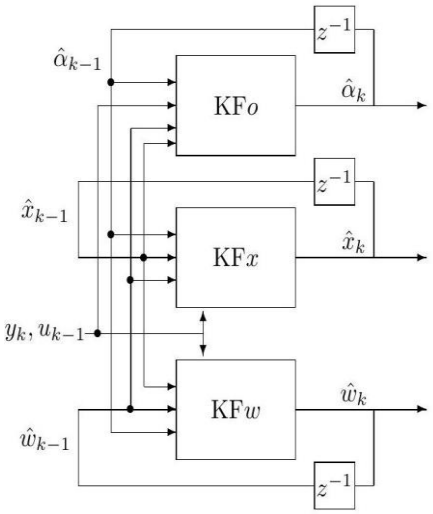

Fig. 1. The triple estimation algorithm scheme

5.1. Order estimation filter KFo

For the order estimation problem, the unscented fractional variable order Kalman filter with finite length differences implementation is used. The order changing dynamics is assumed to be a constant, given by

$$\alpha_{k+1} = \alpha_k + \omega_k^o,$$

where ω_k^o is a noise with variance given by matrix Q_k^o. The matrix Q_k^o represents our knowledge over how big fluctuations in time actually are vis-à-vis those that were assumed by us.

The KFo algorithm equations are given as follows:

$$
\begin{aligned}
\tilde{\alpha}_k &= \hat{\alpha}_{k-1},\\
\tilde{P}_k^o &= \hat{P}_{k-1}^o + Q_{k-1}^o,\\
\tilde{\boldsymbol{\alpha}}_k &= \left[\tilde{\alpha}_k \quad \tilde{\alpha}_k \pm \left(\sqrt{(L+\lambda)\tilde{P}_k^o}\right)_i\right],\\
{}^{\mathcal{A},L}\Delta^{\tilde{\boldsymbol{\alpha}}_{k,i}}\tilde{\chi}_{k,i}^o &= A(\hat{w}_{k-1})\hat{x}_{k-1} + Bu_{k-1},\\
\tilde{\chi}_{k,i}^o &= h^{\tilde{\boldsymbol{\alpha}}_{k,i}}{}^{L}\Delta^{\tilde{\boldsymbol{\alpha}}_{k,i}}\tilde{\chi}_{k,i}^o\\
&\quad -\sum_{j=1}^{L(k)} (-1)^j \binom{\tilde{\boldsymbol{\alpha}}_{k,i}}{j}\hat{x}_{k-j},\\
\tilde{Y}_{k,i}^o &= C\tilde{\chi}_{k,i}^o,\\
\tilde{y}_k^o &= \sum_{i=0}^{2L} W^{(m)}\tilde{Y}_{k,i},\\
P_{y_k y_k}^o &= \sum_{i=1}^{2L} W_i^{(c)}\left[\tilde{\mathcal{Y}}_{i,k} - \tilde{y}_k\right]\left[\tilde{\mathcal{Y}}_{i,k} - \tilde{y}_k\right]^T\\
&\quad + R^o,\\
P_{\alpha_k y_k}^o &= \sum_{i=1}^{2L} W_i^{(c)}\left[\tilde{\alpha}_{i,k} - \tilde{\alpha}_k\right]\left[\tilde{Y}_{i,k} - \tilde{y}_k\right]^T,\\
\mathcal{K}_k^o &= P_{\alpha_k y_k}^o\left(P_{y_k y_k}^o\right)^{-1},\\
\hat{\alpha}_k &= \tilde{\alpha}_k + \mathcal{K}_k^o(y_k - \tilde{y}_k^o),\\
P_k^o &= \hat{P}_k^o - \mathcal{K}_k^o P_{y_k y_k}^o \mathcal{K}_k^o,\\
Q_k^o &= (1-\delta^o)Q_{k-1}^o\\
&\quad + \delta^o(\mathcal{K}_k^o)(y_k - \tilde{y}_k^o)(y_k - \tilde{y}_k^o)^T(\mathcal{K}_k^o)^T,
\end{aligned}
$$

where $\left(\sqrt{(L+\lambda)P_k}\right)_i$ is i-th column of matrix square root (e.g. Cholesky factorisation), L is a dimension of estimated state vector ($2L+1$ is a number of sigma points) and coefficients of unscented transformation W are given by

$$
\begin{aligned}
W_0^{(m)} &= \lambda/(L+\lambda),\\
W_0^{(c)} &= \lambda/(L+\lambda) + (1 - \mathfrak{A}^2 + \mathfrak{B}),\\
W_i^{(m)} &= W_i^{(c)} = 1/(2(L+\lambda)),
\end{aligned}
$$

where $\lambda = \mathfrak{A}^2(L+\kappa) - L$, $\mathfrak{A}$ is a coefficient describing the width of point expansion during the transformation (in the literature, this is obtained in the range $1 \le \mathfrak{A} \le 1e-4$, and is usually denoted as α, but in the present article, since we are using order α, this notation has been changed); κ is an additional scaling coefficient usually chosen as 3 – L; and $\mathfrak{B}$ is a coefficient that corresponds with our knowledge about type of noise, for Gaussian noise is chosen as $\mathfrak{B} = 2$ (in the literature this is usually denoted as β). The δ coefficient is a 'forgetting factor' according to the Robbins–Monro stochastic approximation scheme for estimating the innovations (see Haykin's study [32], p. 240). The initial values of matrix P_0^o represent our a priori knowledge about error in choosing the initial value of order α_0 (we assume that the initial value is different from the original).

5.2. State estimation filter KFx

As the KFx filter, the fractional variable order Kalman filter algorithm with finite length differences implementation is used, and has the following form:

$$
\begin{aligned}
{}_0^{\mathcal{A},L}\Delta_{k+1}^{\hat{\alpha}_k}\tilde{x}_{k+1} &= A(\hat{w}_{k-1})\hat{x}_k + Bu_k,\\
\tilde{x}_{k+1} &= h^{\hat{\alpha}_k}\,{}_0^{\mathcal{A},L}\Delta_{k+1}^{\hat{\alpha}_k}\tilde{x}_{k+1}\\
&\quad - \sum_{j=1}^{L(k)+1} (-1)^j \binom{\hat{\alpha}_k}{j}\hat{x}_{k+1-j},\\
\tilde{P}_k &= \left(h^{\hat{\alpha}_k}A(\hat{w}_{k-1}) + \hat{\alpha}_k\right)P_{k-1}\\
&\quad \left(h^{\hat{\alpha}_k}A(\hat{w}_{k-1}) + \hat{\alpha}_k\right)^T\\
&\quad + Q_{k-1} + \sum_{j=2}^{L(k)} \binom{\hat{\alpha}_k}{j} P_{k-j}\binom{\hat{\alpha}_k}{j}^T,\\
K_k &= \tilde{P}_k C^T\left(C\tilde{P}_k C^T + R_k\right)^{-1},\\
\hat{x}_k &= \tilde{x}_k + K_k(y_k - C\tilde{x}_k),\\
P_k &= (I - K_k C)\tilde{P}_k,
\end{aligned}
$$

where initial conditions are

$$x_0 \in \mathbb{R}^N,\ P_0 = \mathrm{E}[(\tilde{x}_0 - x_0)(\tilde{x}_0 - x_0)^T],$$

and ν_k and ω_k are assumed to be independent with zero expected value.

5.3. Parameters estimation filter KFw

For KFw filter, another unscented fractional variable order Kalman filter with finite implementation of differences is used. The dynamics of parameter-change are also assumed to be constant, given by

$$w_{k+1} = w_k + \omega_k^w,$$

where ω_k^w is a noise with variance given by matrix Q_k^w. The equations of the filter KFw are very similar to those for filter KFo, and the difference is only in the model replica part:

$$
\begin{aligned}
\tilde{w}_k &= \hat{w}_{k-1}\\
\tilde{P}_k^w &= \hat{P}_{k-1}^w + Q_{k-1}^w,\\
\tilde{\mathcal{W}}_k &= \left[\tilde{w}_k \quad \tilde{w}_k \pm \left(\sqrt{(L+\lambda)\tilde{P}_k^w}\right)_i\right],\\
{}^{\mathcal{A},L}\Delta^{\hat{\alpha}_{k-1}}\tilde{\chi}_{k,i}^w &= A\left(\tilde{\mathcal{W}}_{k,i}\right)\hat{x}_{k-1} + Bu_{k-1},\\
\tilde{\chi}_{k,i}^w &= h^{\hat{\alpha}_{k-1}}\,{}_0^{\mathcal{A},L}\Delta^{\hat{\alpha}_{k-1}}\tilde{\chi}_{k,i}^w\\
&\quad - \sum_{j=1}^{L(k)} (-1)^j \binom{\hat{\alpha}_{k-1}}{j}\hat{x}_{k-j}.
\end{aligned}
$$

Resuming the explanation for TEA, it consists of three subfilters requiring separate sets of parameters and initial conditions.Parameters of the order estimation filter KFo are denoted with the upper index ^{o} (e.g. $\tilde{P}_k^o, Q_{k-1}^o$), whereas parameters of KFw are denoted with the upper index ^{w} (e.g., $\tilde{P}_k^w, Q_{k-1}^w$) and parameters of KFx are rendered without an upper index.

6. IDENTIFICATION AND ANALYSIS OF FRACTIONAL VARIABLE ORDER SYSTEM PARAMETERS

Before we apply the finite length triple estimation algorithm to real plant data (noises' estimation of MEMS sensor), we will present the results of some numerical experiments for constant and

sciendo
DOI 10.2478/ama-2023-0025
acta mechanica et automatica, vol.17 no.2 (2023)
Special Issue "Modern Trends in Automation and Robotics in tribute to Professor Tadeusz Kaczorek"

FVO systems. The one state variable discrete state-space system, used in numerical experiments, is given as follows:

$$ {}_{0}^{\mathcal{A},L}\Delta_{k+1}^{\alpha_{k+1}} x_{k+1} = f x_k + u_k + \omega_k \tag{1} $$

$$ x_{k+1} = h^{\alpha_{k+1}} {}_{0}^{\mathcal{A},L}\Delta_{k+1}^{\alpha_{k+1}} x_{k+1} - \sum_{j=1}^{L(k)+1} (-1)^j \binom{\alpha_{k+1}}{j} x_{k-j+1} \tag{2} $$

$$ y_k = x_k + v_k \tag{3} $$

6.1. Analysis of fractional constant and variable order system with input signal known

The number of samples in the numerical implementation of fractional order differences plays a significant role in determining the accuracy of the results. Therefore, in this section, we try to validate the influence of TEA with finite length approximation on final estimation results. We present the TEA with length constraints to make a numerical validation of its capabilities in the analysis of fractional constant and variable order systems. The estimation results were shown for various input signals and order functions. So, the problem in this section is formulated as follows: Estimate the state, order and parameter of the fractional order system with known input signal based on TEA with length constraints. The numerical tests were conducted in the Matlab/Simulink environment based on the Fractional Variable Order Derivative Toolkit [33], with a sample time given as $h = 0.001$ s. The possibilities of the TEA designed with limited length were shown in the Examples (1)–(3). The aim of the examples is to assess the accuracy of the results derived from estimation of the state, order and parameter under various scenarios. The Example (1) deals with the fractional constant order system with input signal being the sawtooth wave, while the Examples (2) and (3) show the behaviour of TEA applied to fractional variable order systems for input signal being the sawtooth wave and Gaussian noise, respectively.

To compare the estimation results for various lengths of TEA implementation, the Examples (1)–(3) were run with the following, individually adjusted parameters:

– Noises parameters

$$ \mathrm{E}[\omega\omega^T] = 10^{-5}, \quad \mathrm{E}[vv^T] = 10^{-3}, $$

– Parameters of KFx filter

$$ P_0 = [1], Q_0 = [10^{-5}], \quad x_0 = [0], R = [10^{-3}], $$

– Parameters of KFo filter

$$ P_0^o = [0.05], Q_0^o = [0.005], \quad \alpha_0 = [1], R^o = [10^{-3}], \quad \mathfrak{A} = 1, \mathfrak{B} = 2, \delta^o = 0.5, $$

– Parameters of KFw filter

$$ P_0^w = [0.001], Q_0^w = [0.01], \quad w_0 = [0], R^w = [10^{-3}], \quad \mathfrak{A} = 1, \mathfrak{B} = 2, \delta^w = 0.5. $$

An identification of the fractional constant order system for various lengths of TEA is presented in Example 1. In this example, the implementation length of TEA is reduced to 50% of the original ones needed to cover a full range of consideration of fractional order system, with no losses in number of samples.

Example 1. Let us consider the DFVOSS $\mathcal{A}$-type system given by Eqs (1)–(3), where

$$ A = f = -0.3, B = 1, C = 1, \alpha_k = 0.6. $$

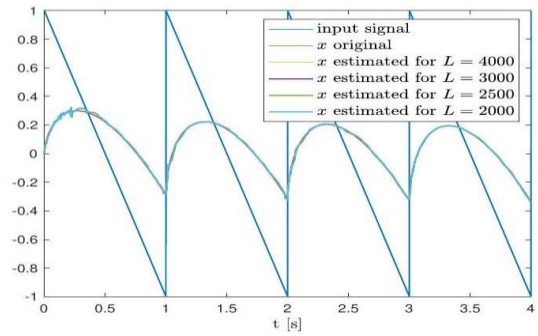

Fig. 2. Original and estimated state variable from Example 1 given for full $(\mathrm{L} = 4{,}000)$ and finite $(\mathrm{L} = 3{,}000,$ $\mathrm{L} = 2{,}500$ and $\mathrm{L} = 2{,}000)$ approximation lengths

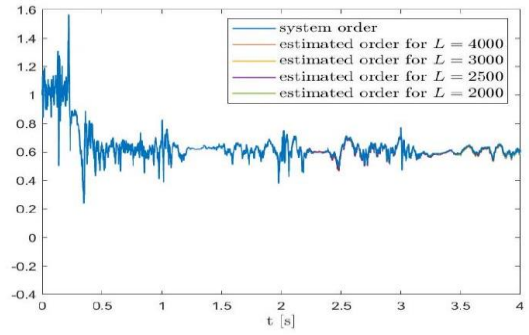

Fig. 3. Original and estimated order from Example 1 given for full $(\mathrm{L} = 4{,}000)$ and finite $(\mathrm{L} = 3{,}000, \mathrm{L} = 2{,}500$ and $\mathrm{L} = 2{,}000)$ approximation lengths

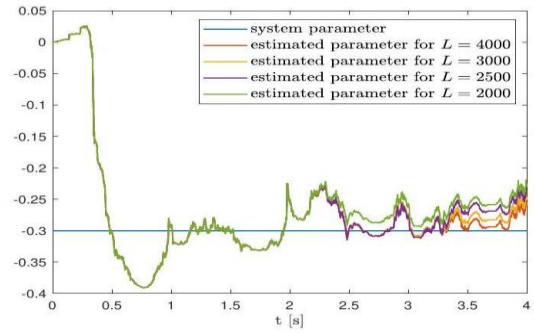

Fig. 4. Original and estimated parameter from Example 1 given for full $(\mathrm{L} = 4{,}000)$ and finite $(\mathrm{L} = 3{,}000, \mathrm{L} = 2{,}500$ and $\mathrm{L} = 2{,}000)$ approximation lengths

The state, order and parameter estimation of the system described in Example 1 are presented in Figs. 2, 3 and 4, respectively. In this example, for all implementation lengths of TEA, the state estimation converges to the original one with high accuracy. Moreover, despite the 50% length reduction of TEA, the order estimations overlap each other and this overlap does not influence the final order results. However, from Fig. 4, it is possible to note

DOI 10.2478/ama-2023-0025

some amount of discrepancy between various tails' implementations of TEA. The plots of the estimated parameters are near the original one, but the differences between them are, in this case, noticeable. All these observations indicate that order estimation is much more robust in reducing samples of number than parameter estimation. We can infer that in pursuance of maintaining the high values of order estimation, even small differences in parameter estimation lead to high accuracy in state estimation.

We achieved satisfying estimation results even with a high percentage length reduction of TEA. Thus, it can also be interesting to show the time execution of TEA depending on its implementation length. The time consumption of the TEA algorithm, depending on its length implementation, is presented in Tab. 1. As we can see, the average execution time of TEA equals around 230 s for a set of 4,000 combined samples of state, order and parameter estimation. On the other hand, for 2,000 samples, the same estimation process took around 184 s. The time-consuming tests were conducted on a PC with an Intel Core i7-5500U CPU, 2.4 GHz, 8 GB RAM and Matlab version 2021b 64 bit. The sum squared error (SSE) of state, order and parameter for various implementation lengths of TEA corresponding to Example 1 is given in Tab. 2. The SSE is calculated as a sum of squares' differences between original data and the corresponding estimates.

Tab. 1. Time execution of TEA depending on its implementation length (L)

Implementation length (L)	Time execution (s)
$L = 4{,}000$	230.75
$L = 3{,}000$	218.76
$L = 2{,}500$	195.30
$L = 2{,}000$	183.55

Tab. 2. The sum squared error of state, order and parameter corresponding to Example 1; for various lengths of TEA

Length	State	Parameter	Order
L=4,000	0.2179	37.8467	62.7249
L=3,000	0.2175	38.1044	62.7476
L=2,500	0.2180	38.6321	62.8327
L=2,000	0.2170	39.8187	62.9066

An estimation of the fractional variable order system is presented in Example 2. It is an extension of Example 1 while replacing the constant value of the order with a time-varying function. In this example, we show the results of applying the TEA with its full implementation range and reduced to 50%.

Example 2. Let us consider the DFVOSS $\mathcal{A}$-type system given by Eqs (1)–(3), where

$A = f = -0.3, B = 1, C = 1,$

$\alpha_k = 0.2 + 0.1kh$ for $k = 1,2,3, \ldots$

In this case, we can see that despite reduced estimation length in TEA, the results tend to be the original values of the desired system. The state, order and parameter estimation are shown in Figs. 5, 6 and 7, respectively. The state estimation is reflected with high accuracy for constraint and unconstraint TEA implementation. The original and both estimated states overlap with high accuracy. Compared to Example 1, the order and parameter estimations achieved the original values starting with 1 s, and maintained these during the whole simulation process. In Figs. 6 and 7, we can observe the only slight difference between the estimation of order and parameter for TEA considering 4,000 and 2,000 historical samples. These insignificant changes and time-consumption reduction show the advantage of the proposed TEA with implementation length constraints. The sum squared error (SSE) of state, order and parameter for various implementation lengths of TEA corresponding to Example 2 is given in Tab. 3.

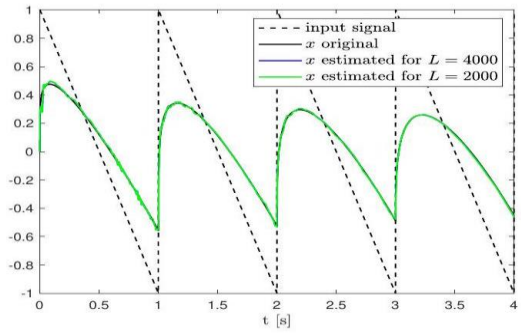

Fig. 5. Original and estimated state variable from Example 2 given for full $(\mathrm{L} = 4{,}000)$ and finite $(\mathrm{L} = 2{,}000)$ approximation lengths

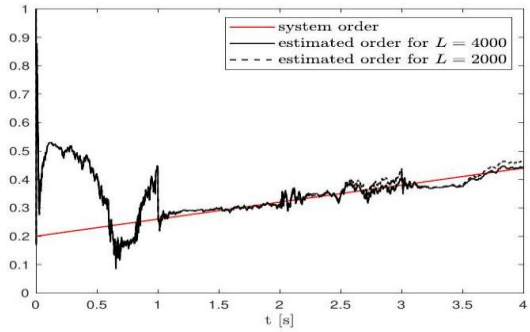

Fig. 6. Original and estimated order from Example 2 given for full $(\mathrm{L} = 4{,}000)$ and finite $(\mathrm{L} = 2{,}000)$ approximation lengths

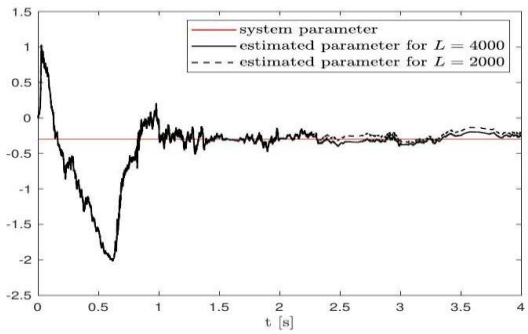

Fig. 7. Original and estimated parameter from Example 2 given for full $(\mathrm{L} = 4{,}000)$ and finite $(\mathrm{L} = 2{,}000)$ approximation lengths

Tab. 3. The sum squared error of state, order and parameter corresponding to Example 2; for various length of TEA

Length	State	Parameter	Order
L=4,000	0.1635	34.8872	1663.2
L=2,000	0.1634	35.0478	1663.1

Usage of the TEA in the estimation process for fractional variable order system with input signal being the Gaussian noise is shown in Example 3. The noise parameters are 0 mean value and 0.1 variance.

DOI 10.2478/ama-2023-0025

Example 3. Let us consider the DFVOSS $\mathcal{A}$-type system given by Eqs (1)–(3), where

$$A = f = -0.3, B = 1, C = 1, u_k \sim \mathcal{N}(0,0.1)$$
$$\alpha_k = 0.2 + 0.1kh \text{ for } k = 1,2,3,\ldots.$$

The estimation results achieved in Example 3 are shown in Figs. 8–10. In contrast with both of the previous examples, there is no difference between state estimation for TEA with length $L = 4{,}000$ vis-à-vis that with length $L = 2{,}000$. Applying the noisy input signal and time-varying order to the TEA lead to the same results for both algorithms' lengths. It is an interesting issue that decreasing the number of samples in TEA reduces its computation time and does not influence results. Fig. 9 shows that the order estimations overlap the original one up to 2.5 s., and starting with this time, the small difference occurs. A similar situation can be observed on the plot with parameter estimation (see Fig. 10), where the curves are near the original ones. The obtained results demonstrate the high precision of TEA for the reduced number of samples applied to fractional variable order systems with Gaussian noise as an input signal. The sum squared error (SSE) of state, order and parameter for various implementation lengths of TEA corresponding to Example 3 is given in Tab. 4.

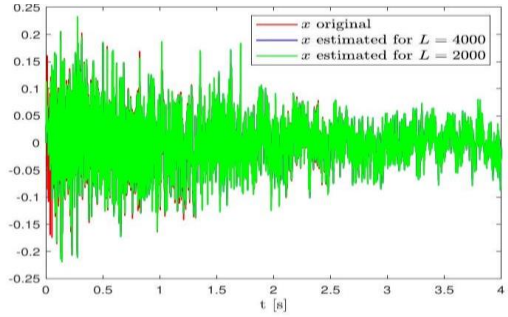

Fig. 8. Original and estimated state variable from Example 3 given for full $(\mathrm{L} = 4{,}000)$ and finite $(\mathrm{L} = 2{,}000)$ approximation lengths

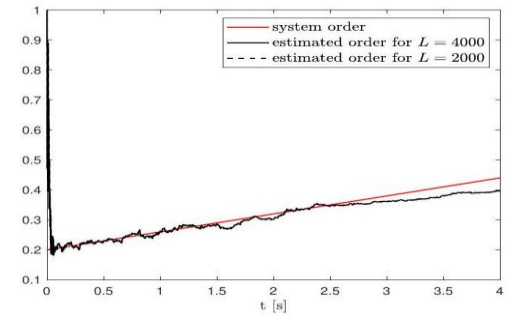

Fig. 9. Original and estimated order from Example 3 given for full $(\mathrm{L} = 4{,}000)$ and finite $(\mathrm{L} = 2{,}000)$ approximation lengths

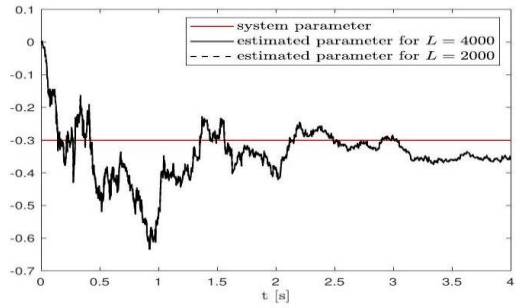

Fig. 10. Original and estimated parameter from Example 3 given for full $(\mathrm{L} = 4{,}000)$ and finite $(\mathrm{L} = 2{,}000)$ approximation lengths

Tab. 4. The sum squared error of state, order and parameter corresponding to Example 3; for various length of TEA

Length	State	Parameter	Order
L=4,000	0.4711	738.2196	1875.8
L=2,000	0.4831	744.9644	1902.9

6.2. Identification without input signal knowledge

When an input signal is not measured, the identification process can differ from desired values or order and system parameter. This can be explained by the fact that in practice, the system noise can have some unknown dynamical correlation of some order and parameter. Let us assume the fractional noise system equation in the following form:

$$\Delta_1^{\alpha} x_{k+1} = f_1 x_k + \omega_k'$$

where ω_k' is a system noise also containing the fractional order dynamical correlation described by the following relation:

$$\Delta_2^{\alpha} \omega_{k+1}' = f_2 \omega_k' + \omega_k$$

where ω_k is assumed to be noise without dynamical correlation.

By combining both equations, we obtain

$$\Delta_1^{\alpha} x_{k+1} - \frac{1}{f_2}\Delta_2^{\alpha}\omega_{k+1}' = f_1 x_k - \frac{1}{f_2}\omega_k.$$

As we can see, this dynamical correlation can have a direct effect on estimated order and system parameter in the estimation process, which can make the obtained estimation results different from those assumed in numerical models, because they consider also the dynamical correlation of the source noise. However, this will not pose a problem in estimation of real plant noise because the aim of estimation is to find the most appropriate model with the assumption that the source noise is without dynamical correlation.

7. IDENTIFICATION AND ANALYSIS OF MEMS GYROSCOPE'S NOISES

Motivated by the study of Macias et al. [24], where it was shown that the accelerometer's noise of MPU9250 contains the fractional order behaviour, we decided to make a noise analysis of its three-axes gyroscope. We utilise the TEA with various approximation lengths during the estimation process. The reduced implementation length of TEA by up to 50% decreases time execution and has an insignificant impact on final estimation results.

This section provides the experimental results pertaining to the modelling of noises for the three-axes gyroscope that forms part of the SparkFun MPU9250 Inertial Measurement Unit (IMU) built-in MEMS technology. We assume unknown input signal knowledge during the entirety of the estimation process.

The MPU9250 unit is a nine degree of freedom MEMS with three accelerometer's axes, three gyroscope's axes and three magnetometer's axes. It breakout board runs on 3.3 VDC and contains $\mathrm{I}^2\mathrm{C}$ and SPI communication protocols.

7.1. Experimental setup

The gyroscope's data were collected based on an experimental setup that is presented in Fig. 11. The Inertial Measure-

ment Unit (IMU), denoted as MPU9250 in a stationary position, was connected to an Arduino Due development board using the $\mathrm{I}^2\mathrm{C}$ protocol. Its operating range was configured to $+/-2{,}000\ \mathrm{dps}$, and the step time for data gathering equals $0.01\ \mathrm{s}$. Then, the measurement noises from the three axes of the gyroscope were transferred to the Matlab/Simulink environment and analysed using the triple estimation algorithm. The estimations of state, order and parameter of noises corresponding to the gyroscope axes x, y and z were conducted based on TEA with full implementation length $(L = 3{,}000)$ and constrained to 50% by setting L to 1,500 considering samples. The TEA was separately applied to noise estimations carried out for the x, y and z axes under, respectively, the following $\mathrm{KF}x$, $\mathrm{KF}o$ and $\mathrm{KF}w$ parameters:

– Parameters of $\mathrm{KF}x$ filter:

$$P_0 = [0.01], Q_0 = [0.15],$$
$$x_0 = [0], R = \begin{cases} 0.0235 & \text{for } x\text{-axis noise} \\ 0.0178 & \text{for } y\text{-axis noise} \\ 0.0191 & \text{for } z\text{-axis noise} \end{cases}$$

– Parameters of KFo filter:

$$P_0^o = [0.01], Q_0^o = [0.1],$$
$$\alpha_0 = [1], \mathfrak{A} = 1, \mathfrak{B} = 2, \delta^o = 0.5,$$
$$R^o = \begin{cases} 0.0235 & \text{for } x\text{-axis noise} \\ 0.0178 & \text{for } y\text{-axis noise} \\ 0.0191 & \text{for } z\text{-axis noise} \end{cases}$$

– Parameters of KFw filter:

$$P_0^w = [0.01], Q_0^w = [0.1],$$
$$w_0 = [0], \mathfrak{A} = 1, \mathfrak{B} = 2, \delta^w = 0.5,$$
$$R^w = \begin{cases} 0.0235 & \text{for } x\text{-axis noise} \\ 0.0178 & \text{for } y\text{-axis noise} \\ 0.0191 & \text{for } z\text{-axis noise} \end{cases}$$

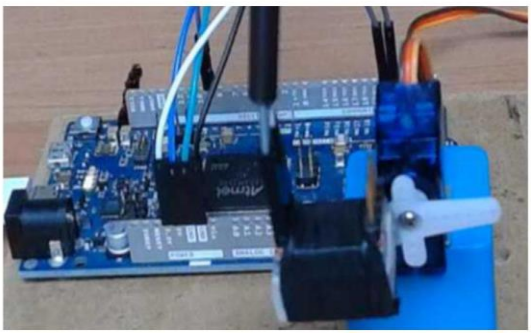

Fig. 11. The real view of experimental setup with an Arduino Due development board and MPU9252 IMU mounted on the shaft of a servo motor in a fixed position

7.2. Experimental results

The estimation of x-axis noise is presented in Fig. 12. It is worth noting that the results overlap with no differences for both lengths of TEA. The state, order and parameter plots are the same despite significant TEA length reduction. Moreover, Fig. 13 confirms, in this case, the fractional order noise, which tends to 0.3. The parameter estimation stabilises its value around -1.6 (see Fig. 14). Collectively, all these observations suggest that the estimation results of x-axis noise are characterised by a high degree of precision.

Analysis of y-axis noise is presented in Figs. 15-17. As shown in Fig.15, the state estimation is well-reflected for both lengths of TEA. In this case, the noise also exhibits the fractional order dynamic, and its order value goes to 0.3 rapidly (see Fig. 16). This order value was maintained until the final estimation process. Additionally, it can be noted in Fig. 17 that the estimated parameter tends to the value -1.5 and follows it with minor fluctuations.

The identification of z-axis noise is shown in Fig. 18. As in previous cases, the constraints of TEA implementation length do not influence estimation results. The order estimation shown in Fig. 19 reveals its fractional behaviour. We can see that this time also, the order value achieved the central value very quickly and stabilises itself around the value 0.3. The parameter estimation of y-axis noise presented in Fig. 20 attains the value -2 in approximately 5 s.

To summarise, using TEA during the noise estimation process allows us to obtain high-accuracy noise models for the x, y and z axes of the gyroscope that forms part of the MPU9250 sensor. Moreover, all the investigated data highlight its fractional order dynamic correlation and robustness for the length constraint of TEA up to 50%. This fact can significantly reduce the time consumption for TEA execution in the absence of estimation of precision losses. The sum squared error (SSE) of state, order and parameter for various implementation lengths of TEA corresponding to experimental data are given in Tab. 5. In this case, the SSE is calculated directly between their estimates for lengths L = 3,000 and L = 1,500.

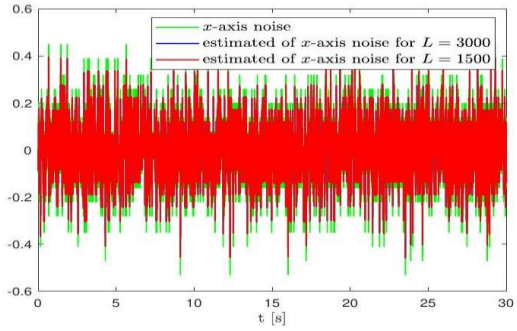

Fig. 12. Original and estimation of x-axis noise given for full $(\mathrm{L} = 3{,}000)$ and finite $(\mathrm{L} = 1{,}500)$ approximation lengths

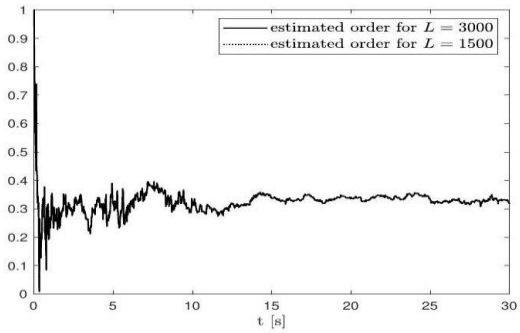

Fig. 13. Order estimation for x-axis noise given for full $(\mathrm{L} = 3{,}000)$ and finite $(\mathrm{L} = 1{,}500)$ approximation lengths

DOI 10.2478/ama-2023-0025

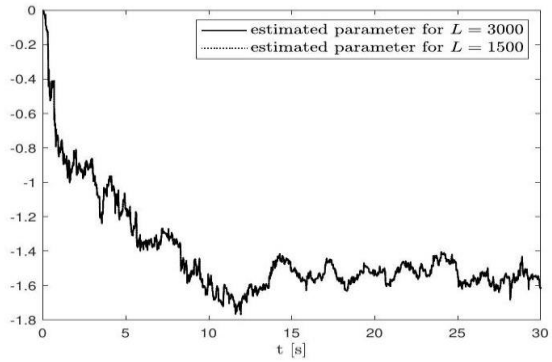

Fig. 14. Parameter estimation for x-axis noise given for full $(\mathrm{L} = 3{,}000)$ and finite $(\mathrm{L} = 1{,}500)$ approximation lengths

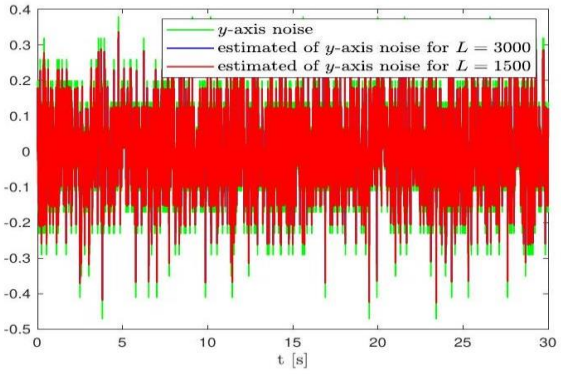

Fig. 15. Original and estimation of y-axis noise given for full $(\mathrm{L} = 3{,}000)$ and finite $(\mathrm{L} = 1{,}500)$ approximation lengths

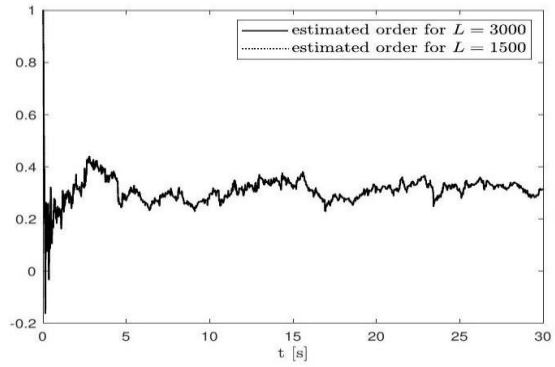

Fig. 16. Order estimation for y-axis noise given for full $(\mathrm{L} = 3{,}000)$ and finite $(\mathrm{L} = 1{,}500)$ approximation lengths

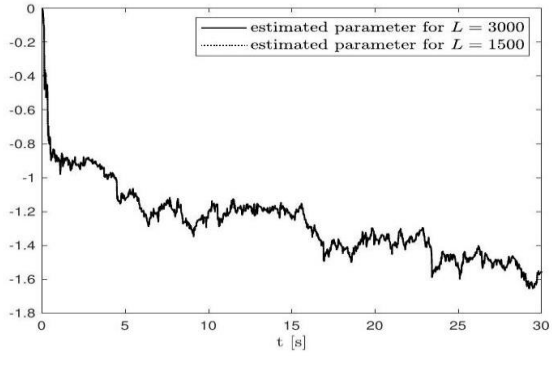

Fig. 17. Parameter estimation for y-axis noise given for full $(\mathrm{L} = 3{,}000)$ and finite $(\mathrm{L} = 1{,}500)$ approximation lengths

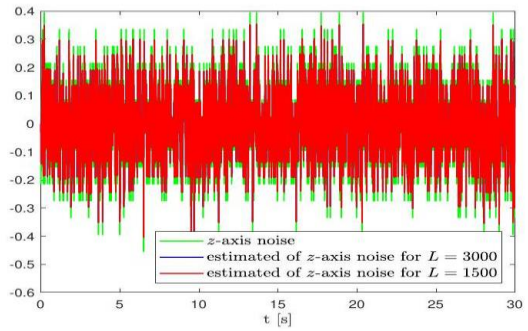

Fig. 18. Original and estimation of z-axis noise given for full $(\mathrm{L} = 3{,}000)$ and finite $(\mathrm{L} = 1{,}500)$ approximation lengths

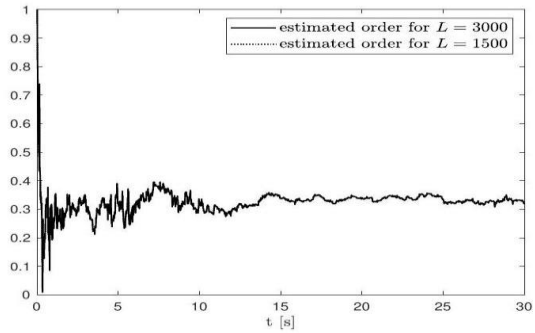

Fig. 19. Order estimation for z-axis noise given for full $(\mathrm{L} = 3{,}000)$ and finite $(\mathrm{L} = 1{,}500)$ approximation lengths

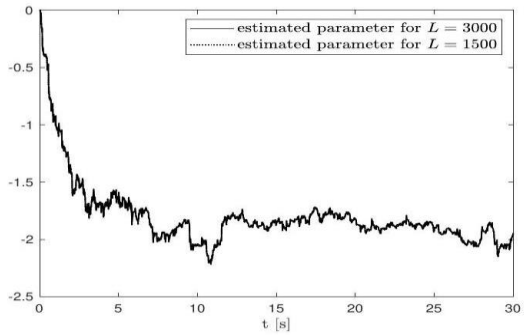

Fig 20. Parameter estimation for z-axis noise given for full $(\mathrm{L} = 3{,}000)$ and finite $(\mathrm{L} = 1{,}500)$ approximation lengths

Tab. 5. The sum squared error of state, order and parameter corresponding to experimental noise data

Noise	State	Parameter	Order
x-axis	$1.79 \cdot 10^{-8}$	$2.16 \cdot 10^{-7}$	$5.09 \cdot 10^{-8}$
y-axis	$3.29 \cdot 10^{-8}$	$2.52 \cdot 10^{-5}$	$1.08 \cdot 10^{-6}$
z-axis	$6.52 \cdot 10^{-9}$	$1.62 \cdot 10^{-6}$	$7.36 \cdot 10^{-8}$

8. CONCLUSIONS

The paper presents the experimental and numerical results of applying the triple estimation algorithm with approximation length constraints. The possibilities of such algorithms have been revealed during the state, order and parameter estimation of fractional constant and variable order systems in several numerical examples. In sets of numerical examples, the implementation length of TEA was reduced to 50% of the number of samples

needed to cover the whole computing range with no implementation losses. The estimated state and order plots for the fractional constant order system tend to the original values. Only a tiny discrepancy occurs during parameter estimation for selective implementation length reduction. However, it has not influenced the final state estimation results. When identifying the fractional variable order system with different lengths of TEA, we can notice only a slight difference between the order estimations. Despite a length reduction to 50% of the original size, the estimated state, order and parameter curves overlap and are near the original ones. The numerical tests confirm the high accuracy of the achieved estimation results even for a finite length of the triple estimation algorithm. Combining numerical results leads to the conclusion that a reduction of samples by up to 50% does not significantly affect the state estimation results of considering fractional order systems and substantially decreases its time duration.

The triple estimation algorithm was also successfully used for fractional noise estimation of the gyroscope, part of a popular Inertial Measurement Unit known as MPU9250. The noise analysis was conducted for x, y and z axes of the gyroscope. The state, order and parameter estimation results for each axis of the gyroscope are similar. The conducted experiments show that the order of noises for the three gyroscopes' axes equals approximately 0.3, and the estimated parameters achieve a value of around –1.8. At this time, the approximation length also does not influence the final estimation results. Moreover, the experiments show the fractional order correlation dynamics of the investigated noises.

The plethora of numerical examples and experiments allow us to ascertain that the triple estimation algorithm with finite length approximation becomes a convenient tool during the analysis, identification and estimation of fractional variable order systems.

REFERENCES

1. Samko SG, Kilbas AA, Maritchev OI. Fractional Integrals and Derivative. Theory and Applications. Gordon & Breach Sci. Publishers; 1987.
2. Miller KS, Ross B. An Introduction to the Fractional Calculus and Fractional Differenctial Equations. New York, USA: John Wiley & Sons Inc.; 1993.
3. Monje CA, Chen Y, Vinagre BM, Xue D, Fe-liu V. Fractional-order Systems and Controls.London. UK: Springer; 2010.
4. Podlubny I. Fractional Differential Equations. Academic Press; 1999.
5. Magin R, Ortigueira MD, Podlubny I, Trujillo J. On the fractional signals and systems. Signal Processing. 2011;91(3):350 371. Advances in Fractional Signals and Systems.
6. Kilbas AA, Srivastava HM, Trujillo JJ. Theory and Applications of Fractional Differential Equations, Volume 204 (North-Holland Mathematics Studies). USA: Elsevier Science Inc. 2006.
7. West BJ. Fractional Calculus and the Future of Science. Entropy. 2021;23(12). https://www.mdpi.com/1099-4300/23/12/1566
8. Anastassiou GA. Generalized Fractional Calculus. Springer. Cham. 2021.
9. Yang XJ. General Fractional Derivatives: Theory, Methods and Applications. Chapman and Hall/CRC; 2019.
10. Tarasov VE. Generalized Memory: Fractional Calculus Approach. Fractal and Fractional. 2018;2(4).https://www.mdpi.com/2504-3110/2/4/23.
11. Sierociuk D, Dzielinski A, Sarwas G, Petras I, Podlubny I, Skovranek T. Modelling heat transfer in heterogeneous media using fractional calculus. Philosophical Transactions of the Royal Society A: Mathematical, Physical and Engineering Sciences. 2013;371(1990).
12. Sakrajda P, Sierociuk D. Modeling Heat Transfer Process in Grid-Holes Structure Changed in Time Using Fractional Variable Order Calculus. In: Babiarz A, Czornik A, Klamka J, Niezabitowski M, editors. Theory and Applications of Non-integer Order Systems. Cham: Springer International Publishing. 2017: 297-306.
13. Reyes-Melo ME, Martinez-Vega JJ, Guerrero-Salazar CA, Ortiz-Mendez U. Application of fractional calculus to modelling of relaxation phenomena of organic dielectric materials. In: Proceedings of International Conference on Solid Dielectrics. Toulouse. France: 2004.
14. Dzielinski A, Sierociuk D, Sarwas G. Some applications of fractional order calculus. Bulletin of The Polish Academy of Sciences – Technical Sciences. 2010;58(4):583-92.
15. Ortigueira MD, Val´erio D. Fractional Signals and Systems. De Gruyter; 2020. https://doi.org/10.1515/9783110624588.
16. Sheng H, Chen Y, Qiu T. Fractional Processes and Fractional-Order Signal Processing. Springer. London; 2012.
17. Muresan CI, Birs IR, Dulf EH, Copot D, Miclea L. A Review of Recent Advances in Fractional-Order Sensing and Filtering Techniques. Sensors. 2021;21(17). Available from: https://www.mdpi.com/1424-8220/21/17/5920.
18. Sierociuk D, Tejado I, Vinagre BM. Improved fractional Kalman filter and its application to estimation over lossy networks. Signal Processing. 2011 MAR;91(3, SI):542-52.
19. Sierociuk D. Fractional Kalman Filter algorithms for correlated system and measurement noises. Control and Cybernetics. 2013;42(2):471-90.
20. Sierociuk D, Ziubinski P. Variable order fractional Kalman filters for estimation over lossy network. Lecture Notes in Electrical Engineering. 2015;320:285-94.
21. Wyss W. Fractional noise. Foundations of Physics Letters. 1991;4: 235–246.
22. Sierociuk D, Ziubinski P. Fractional order estimation schemes for fractional and integer order systems with constant and variable fractional order colored noise. Circuits, Systems, and Signal Processing. 2014;33(12):3861-82. DOI:10.1007/s00034-014-9835-0.
23. Sierociuk D, Macias M. Triple Estimation of Fractional Variable Order, Parameters, and State Variables Based on the Unscented Fractional Order Kalman Filter. Sensors. 2021;21(23). Available from: https://www.mdpi.com/1424-8220/21/23/8159.
24. Macias M, Sierociuk D, Malesza W. MEMS Accelerometer Noises Analysis Based on Triple Estimation Fractional Order Algorithm. Sensors. 2022;22(2).
25. Stanislawski R, Latawiec KJ, Lukaniszyn M, Galek M. Time-domain approximations to the Grunwald-Letnikov difference with application to modeling of fractional-order state space systems. In: 2015 20th International Conference on Methods and Models in Automation and Robotics (MMAR). 2015: 579-84.
26. Stanislawski R, Hunek WP, Latawiec KJ. Finite approximations of a discrete-time fractional derivative. In: 2011 16th International Conference on Methods Models in Automation Robotics. 2011:142-5.
27. Sierociuk D, Malesza W, Macias M. Derivation, interpretation, and analog modelling of fractional variable order derivative definition. Applied Mathematical Modelling. 2015;39(13):3876-88. http://dx.doi.org/10.1016/j.apm.2014.12.009.
28. Sierociuk D, Malesza W, Macias M. On the Recursive Fractional Variable-Order Derivative: Equivalent Switching Strategy, Duality, and Analog Modeling. Circuits, Systems, and Signal Processing. 2015;34(4):1077-113.
29. Macias M, Sierociuk D. An alternative recursive fractional variable-order derivative definition and its analog validation. In: Proceedings of International Conference on Fractional Differentiation and its Applications. Catania, Italy; 2014.

30. Ziubinski P, Sierociuk D. Fractional order noise identification with application to temperature sensor data. In: Circuits and Systems (ISCAS), 2015 IEEE International Symposium on; 2015: 2333-6.
31. Sierociuk D, Malesza W. Fractional variable order discrete-time systems, their solutions and properties. International Journal of Systems Science. 2017;48(12):3098-105.
32. Haykin S. Kalman Filtering and Neural Networks. John Wiley & Sons, Inc.: New York, USA; 2001.
33. Sierociuk D. Fractional Variable Order Derivative Simulink Toolkit; 2012. http://www.mathworks.com/matlabcentral/fileexchange/38801-fractional-variable-order-derivative-simulink-toolkit
34. Wu B, Cao X. Robust Attitude Tracking Control for Spacecraft with Quantized Torques. IEEE Transactions on Aerospace and Electronic Systems. 2017;11:1-1.
35. Wang Y, Yang X, Yan H. Reliable Fuzzy Tracking Control of Near-Space Hypersonic Vehicle Using Aperiodic Measurement Information. IEEE Transactions on Industrial Electronics. 2019;66(12):9439-47.
36. Sulochana S, Hablani H. Precision Munition Guidance and Moving-Target Estimation. Journal of Guidance, Control, and Dynamics. 2016;39:1-12.
37. Xingling S, Shi Y, Wendong Z. Input-and-Measurement Event-Triggered Output Feedback Chattering Reduction Control for MEMS Gyroscopes. IEEE Transactions on Systems, Man,and Cybernetics: Systems. 2021.
38. Xingling S, Shi Y, Wendong Z, Cao H, Jiawei L. Neurodynamic Approximation-Based Quantized Control with Improved Transient Performances for MEMS Gyroscopes: Theory and Experimental Results. IEEE Transactions on Industrial Electronics. 2020.
39. Xingling S, Shi Y. Neural-Network-Based Constrained Output-Feedback Control for MEMS Gyroscopes Considering Scarce Transmission Bandwidth. IEEE Transactions on Cybernetics. 2022.
40. Xingling S, Si H, Zhang W. Fuzzy wavelet neural control with improved prescribed performance for MEMS gyroscope subject to input quantization. Fuzzy Sets and Systems. 2020;411.

Michał Macias: https://orcid.org/0000-0001-7123-7708

Dominik Sierociuk: https://orcid.org/0000-0002-3700-3665